Chalcogenide Letters Vol. 11, No. 12, December 2014, p. 629 - 638

EFFECT OF ANNEALING ON THE PROPERTIES OF CHEMICAL BATH DEPOSITED CdS BUFFER LAYER OF CIS SOLAR CELLS

F. I. EZEMA[a,b,c,d*], Y. KAYAMA[d], I. C. AMAECHI[a], T. HIRAMATSU[d], A. C. NWANYA[a,f], R. U. OSUJI[a,b,c], M. MALIK[b,c], M. SUGIYAMA[d]

[a]*Department of Physics and Astronomy, University of Nigeria, Nsukka – Enugu State, Nigeria*

[b]*Nanosciences African Network (NANOAFNET), iThemba LABS-National Research Foundation, 1 Old Faure road, Somerset West 7129, POBox 722, Somerset West, Western Cape Province, South Africa*

[c]*UNESCO-UNISA Africa Chair in Nanosciences/Nanotechnology, College of Graduate Studies, University of South Africa (UNISA), Muckleneuk ridge, POBox 392, Pretoria-South Africa*

[d]*Department of Electrical Engineering, Faculty of Science and Technology, Tokyo University of Science, 2641 Yamazaki, Noda 278-8510, Japan*

[f]*National Center for Energy Research and Development, University of Nigeria, Nsukka*

The effect of annealing on the properties of chemical bath deposited (CBD) cadmium sulfide (CdS) buffer layer $CuInS_2$ (CIS) solar cell with respect to cell performance is reported. The CdS layer was deposited on the CIS film from CdI_2 and thiourea $[CS(NH_2)_2]$ solutions using ammonia as the complexing agent. Results showed that post-conditional process of chemical bath deposition of CdS layer affected the performance of the CIS solar cells. X-ray diffraction (XRD) results indicated that CdS buffer layers show a hexagonal structure with preferred orientation along the (101) axis without $Cd(OH)_2$ peak at 200^{o}C. The morphologies of CdS films were investigated using scanning electron microscopy (SEM) and atomic force microscopy (AFM). The performance of the CdS/CIGS solar cells was discussed on the basis of characteristics and post-deposition conditions of the chemical bath deposited CdS layer.

(|Received October 23, 2014; Accepted December 3, 2014)

Keywords: Chemical bath deposition (CBD), Cadmium sulfide (CdS), Buffer layer $CuInS_2$ (CIS), solar cell

1. Introduction

$Cu(In,Ga)S_2/Se_2$ (CIGS) has proved a promising material in the quest for sustainable and high efficiency materials for thin film solar cells. So far, cadmium telluride (CdTe) and copper–indium–sulfide (CIS) solar cells with CdS as window layer has shown efficiencies close to 12% and 16% respectively [1,2]. CIS photovoltaic modules have become attractive because they are stable, relatively cheaper, have short payback time, are adaptable to various applications and have a large supporting research and development community [3]. CIGS have also shown high efficiencies close to 20.4% [4].

The $CuInS_2$ absorber in a solar cell is typically prepared by sequential deposition of Cu and In metallic layers (i.e. a Cu/In bilayer) on Mo/glass substrate by vacuum methods such as sputtering and evaporation [5–7], followed by sulfurization [5–11]. However, these methods require expensive equipment, high temperature and pressure and a significant loss of raw materials [12]. In an attempt to reduce these shortcomings, some non-vacuum methods such as spraying

* Corresponding author: fiezema@yahoo.com

[13–16] and electrochemical deposition [17–19], have been used. One of the critical problems of electrochemical deposition of Cu/In film is the difficulty in obtaining a homogeneous In layer, i.e. the In layer tends to form an island-shaped morphology using typical electrochemical deposition solutions based on both chloride and sulfate solutions [20,21]. Metal-organic sulfides, such as dimethylsulfide, diethylsulfide, and ditertiarybutylsulfide [(t-C4H9)2S: DTBS] have attracted much attention as alternative candidates for the source of Sulfate ion [22].

In thin-film CIS solar cell, the p-type CIS film absorbs most of the light and generates the photocurrent [23] while the p-n heterojunction is formed by depositing a thin n-type buffer layer typically CdS on the CIS [24]. Cadmium sulfide (CdS) exhibits n-type semiconductivity with Bhor atomic radius of 2.4 nm and direct band gap (Eg) ≈ 2.4 eV. Due to its excellent properties, CdS is used in many applications such as solar photovoltaic cell and light emitting diodes in flat panel displays [25]. Moreover, reports have shown that CdS is highly reproducible, stable and a cost effective material for the photovoltaic industry [26–28]. The as-grown CdS film may absorb significant amount of water from the environment which degrades the quality of the film [23], hence the need to anneal the films. The effect of heat treatment on CdS/CIGS interfaces in air and various atmospheres has been reported [29, 30].

In this paper, we study the effect of annealing on the optical, structural and solar cell performance of CdS thin film deposited by simple chemical bath deposition (CBD) method on magnetron sputtered $CuInS_2$ films to form CdS/CIS solar cell. CBD method has become more and more popular due to its relatively low-cost requirements, convenience, large area of deposition and easy adaptability [31]. The method has also been satisfactorily applied in regions where availability and affordability of highly sophisticated techniques pose great problems to researchers. The bath temperature, solvent type and particle size may significantly affect the solubility product. However, spontaneous precipitation is eliminated in order for thin films to form by using complexing agent which slowly releases the metal ions on dissociation, resulting in slow deposition of the compound in the chemical bath by ion-ion reaction [32].

The morphology and crystalline structure of CdS at different isothermal conditions was characterized with atomic force/scanning electron microscopy (AFM/SEM) and X-ray diffraction.

2. Experimental details

2.1 Materials

For deposition of cadmium sulfide (CdS) thin film, the bath content was made up of cadmium iodide (CdI_2) as a source of Cd^{2+}, thiourea [$(NH_2)_2CS$], a sulfiding agent and ammonia (NH_3) solution. All the chemical reagents used were of analytical grade. The typical deposition bath consists of 3ml of 1M CdI_2, 5ml of NH_3 and 5ml of 1M thiourea solution. The homogeneous solution was kept at room temperature for 6hrs, after which the coated substrates were removed, rinsed with distilled water and allowed to dry. Later, the CdS films were thermally treated at 100, 200 and 300^{o}C for 30mins in air atmosphere.

Approximately 500-700 nm thickness of Cu-In metallic layers were deposited successively on Mo-coated soda lime glass (Mo/SLG) by RF magnetron sputtering using a Cu-In alloy target without intentionally heating Mo/SLG. Sulfurization of as-deposited Cu-In layer films to form $CuInS_2$ films were performed using the precursor, ditertiarybutylsulfide [$(t\text{-}C_4H_9)_2S$: DTBS] under atmospheric pressure. The flow rates of DTBS and N_2 carrier gas were 35 μmol/min and 2L/min respectively. Fig.1a and b show sulfurization equipment and the heating profile.

For evaluation of the solar cell properties of $CuInS_2$ films, the films were layered to form an ITO/i-ZnO/CdS/CIS/Mo/SLG structure. On the $CuInS_2$ films, a CdS buffer layer was deposited by chemical bath deposition (CBD) discussed above. An i-ZnO and ITO window layer was then deposited on the top of the CdS layer by radio frequency (RF) magnetron sputtering with thicknesses of about 100nm and 500nm respectively.

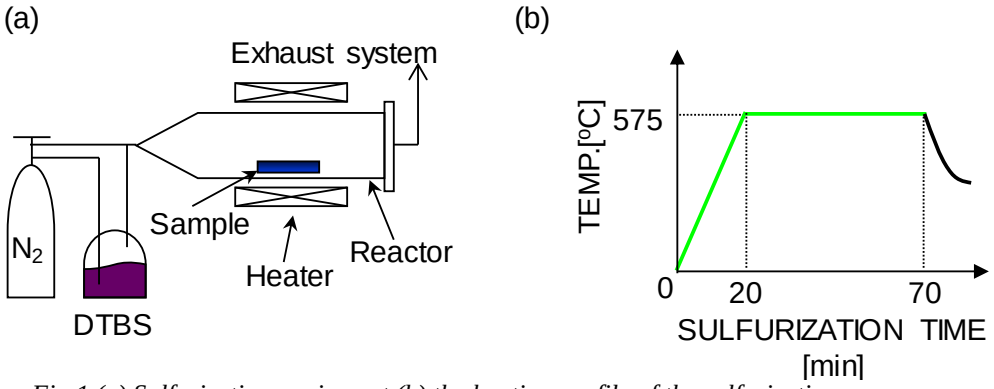

Fig.1 (a) Sulfurization equipment (b) the heating profile of the sulfurization process

2.2 Characterization

Surface morphologies of CdS/CIS films were examined using Hitachi Miniscope TM-1000 scanning electron microscope and Veeco Tapping mode atomic force microscope. X-ray diffraction (XRD) patterns were recorded using Rigaku Ultima IV X-ray diffractometer at 2θ angle between 10^o and 80^o. For optical absorption studies of the films, absorption spectra were taken within the wavelength range 300–2000 nm using Hitachi U-4100 Spectrophotometer.

3. Results and discussion

3.1 Structural analysis

Fig. 2 shows the XRD patterns of CdS films before and after heat treatment at various conditions. The identification, assignment of peaks and preferred orientation were made using JCPDS data card. It was observed that the X-ray diffraction of CdS did not show much variation in peaks after annealing due to the very thin CdS layer. However, it showed that the films have highly oriented crystals with classical hexagonal structure of wurzite type. The (101) reflection at 28.5^o belongs to the hexagonal phase of CdS and appeared in both the annealed and unannealed films.

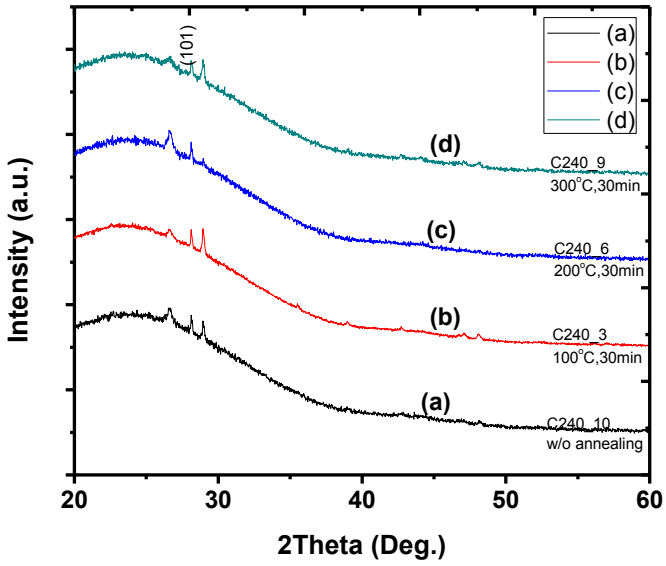

Fig. 2: X-ray diffractograms of both annealed and unannealed of CdS buffer layer at various conditions.

However, there was an extension of peak for hexagonal CdS which was remarkably evident near $2\theta \approx 50^{o}$ for the XRD pattern labeled C240-3 against the mixture of both cubic and hexagonal structure of CdS as claimed by Han et al [33]. The reduction in intensity at higher temperature suggests a phase transformation with evidence that $Cd(OH)_2$ peak was not detected in the diffraction pattern at $200^{o}C$.

3.2 Morphological Characterization and Energy Dispersive Spectroscopy EDS

The surface morphologies of annealed and unannealed CdS were studied by AFM as shown in fig. 3(a-b). The 2D AFM morphological data reveal that both films are composed of agglomerate of grains with different sizes and shapes. The slight porous nature of films could aid ion diffusion. No pinholes and cracks on grain boundaries were observed. From the AFM images, the roughness for both films was found to be 16.4 and 28.8 nm respectively. It was evident that thermal treatment has effect on the morphology and may be the reason for the reduction in open circuit voltage and fill factor for the solar cell. Even though the Cd diffusion property which is indispensible for designing a CIS solar is indeterminable for now, it is strongly influenced not only by the surface morphology of CIS layer but also intrinsic defect properties of the semiconductor. The SEM images with magnification x10,000 (see fig. 4a-d) corroborate the AFM results. Both films consist of network of grains which are scanty over the surface area. However, the consistency in morphologies suggests uniformity in growth with large grains of about 10μm in breadth.

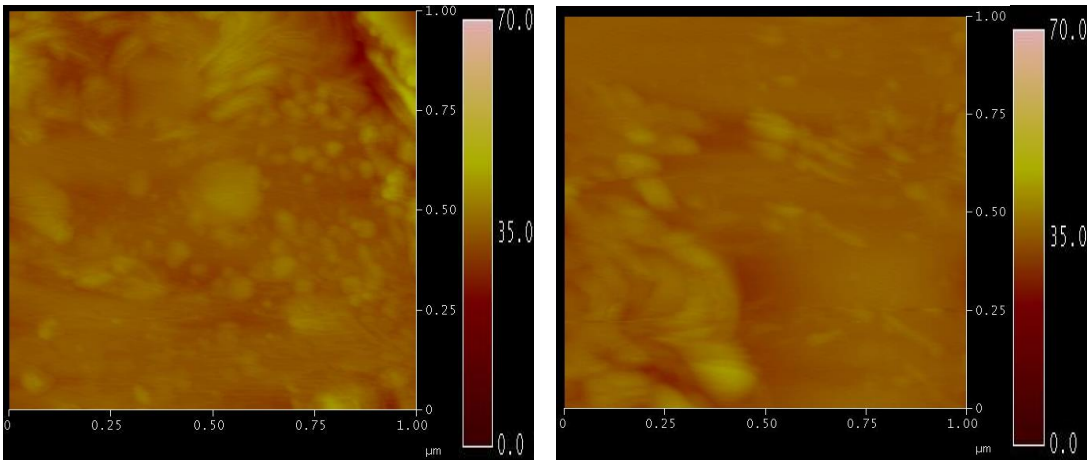

Fig. 3: AFM images of unannealed and annealed CdS buffer layer

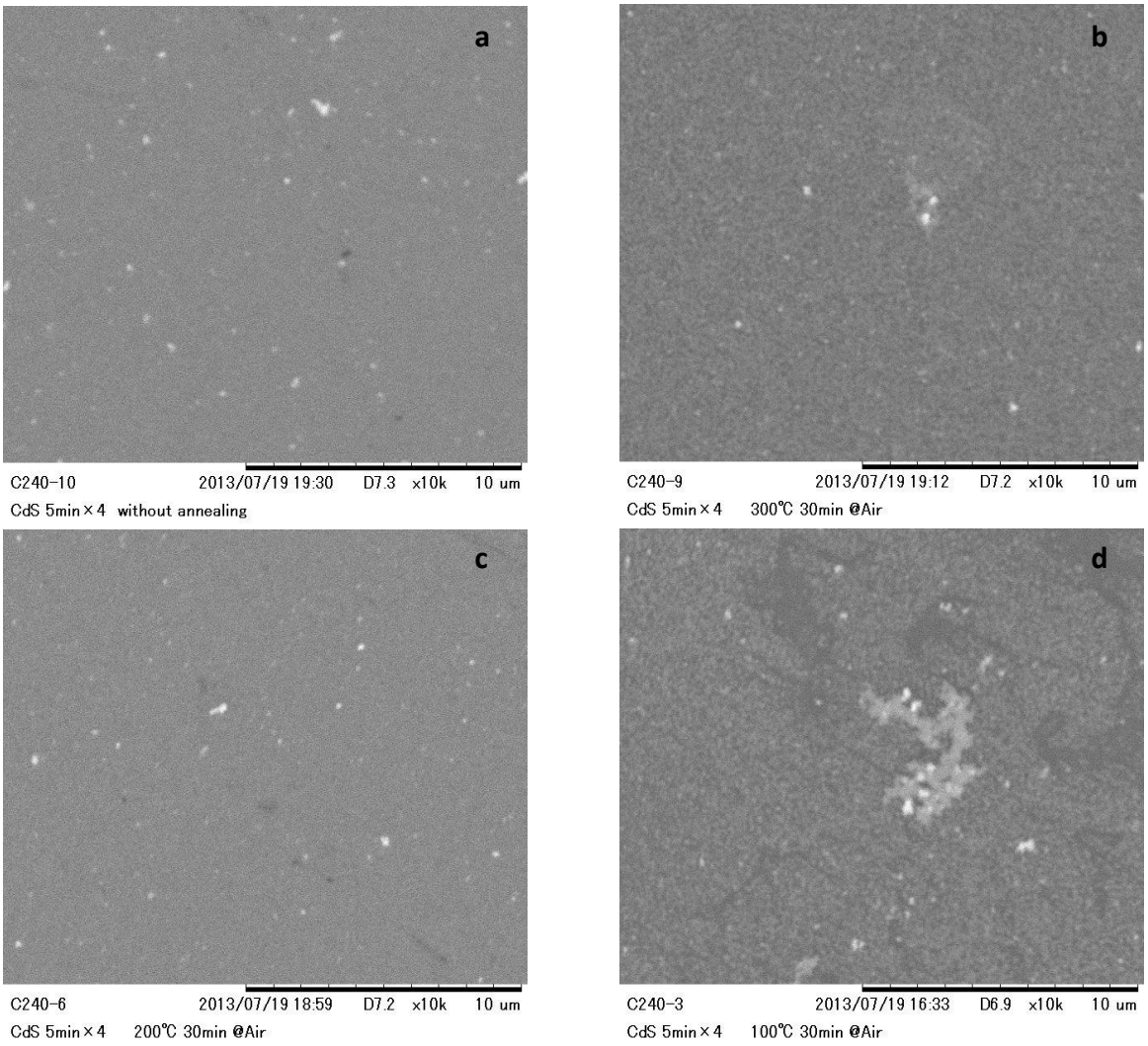

Fig.4: SEM images of CdS buffer layer (a) without annealing (b) annealed at 300^{o}C for 30min (c) annealed at 200^{o}C for 30min (d) annealed at 100^{o}C for 30min.

The EDS spectrum of CdS is as shown in figure 5(a-d). The figure indicates the presence of cadmium and sulfur at the appropriate energy levels. The atomic weight percent of the elements shows that the film was stoichiometric with proportionate combination of elemental Cd and S.

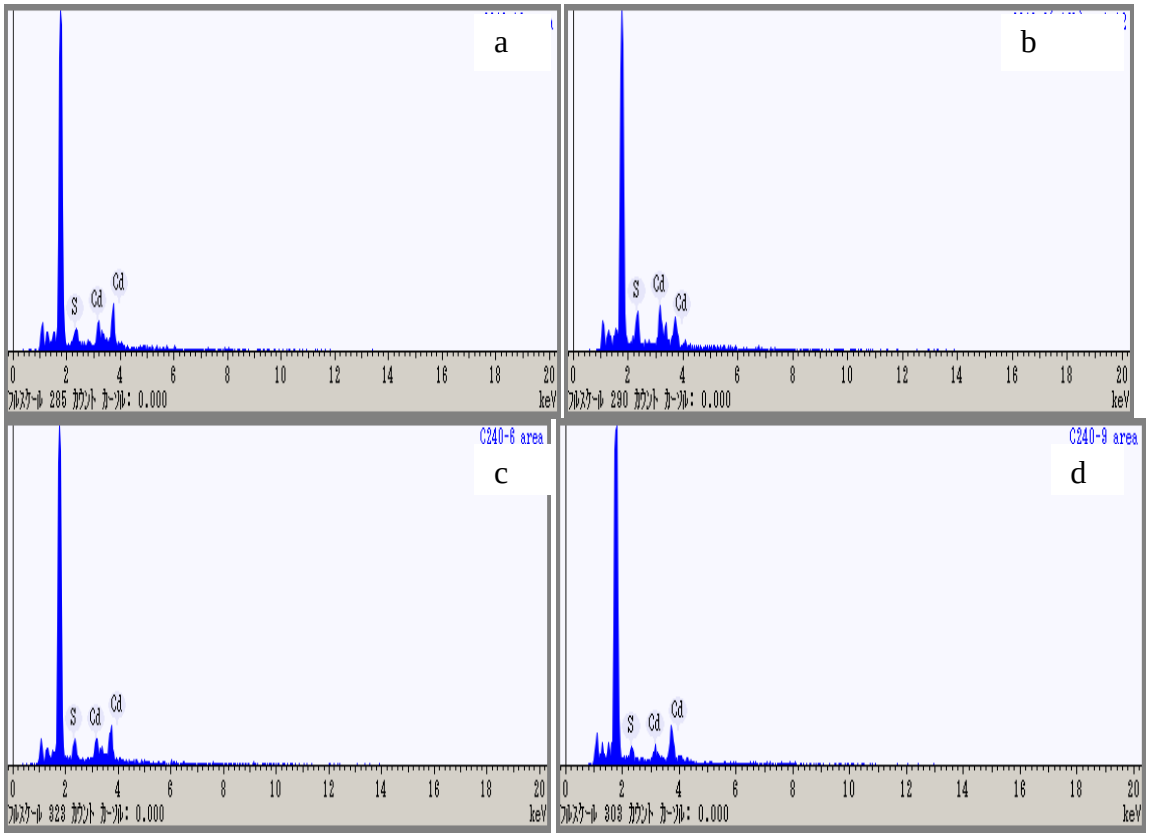

Fig 5: The EDS spectrum of the deposited CdS (a) without annealing (b) annealed at 300^{o}C for 30min (c) annealed at 200^{o}C for 30min (d) annealed at 100^{o}C for 30min

3.3 Optical properties of CdS buffer layer

The optical properties and possible electronic transitions of CdS buffer layer for thin film solar cell were determined from the recorded transmission and reflection spectra. The room temperature optical transmittance recorded in wavelength range 300-2000nm is shown in fig. 6a. The film shows a good optical properties with a well defined electronic transition corresponding to the energy gap of CdS and high transmittance greater than 80% for wavelength in near infrared (NIR) and infrared (IR). Such high transmittance has also been recorded by Rusu et al [34].

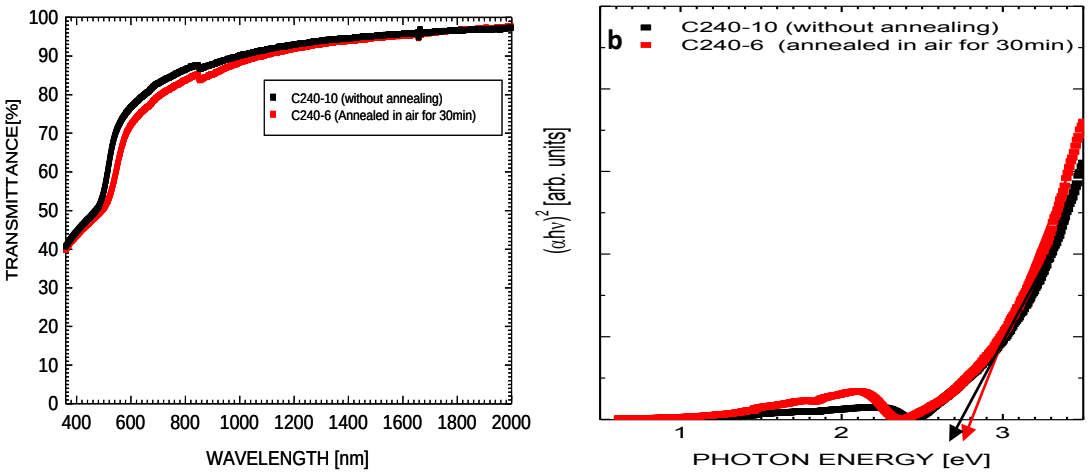

Fig. 6: (a) The spectral transmittance of CdS with and without annealing. (b) Direct energy band gap of annealed and unannealed CdS buffer layer.

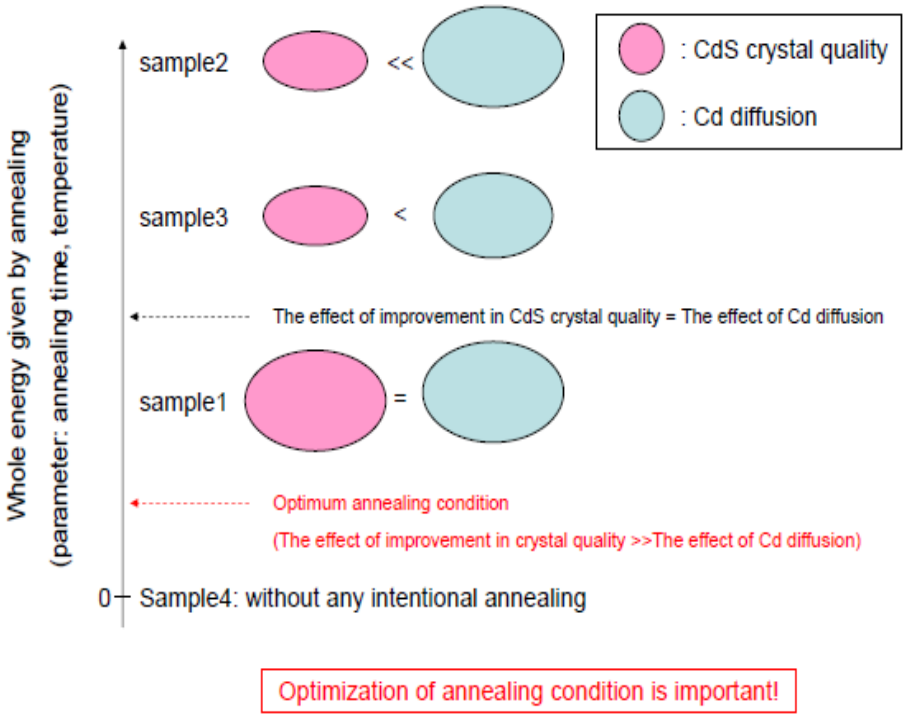

Fig.7. Schematic illustration of efficiency of the cells based on crystalline quality and ion diffusion of cadmium.

Transmission and reflection data were used for the calculation of absorption coefficient, α. The fundamental absorption which corresponds to electronic excitation from the valence band to conduction band can be used to determine the nature and value of optical band gap. Fig. 6b shows the direct energy band gap of CdS layer with and without annealing. The relationship between absorption coefficient, α and incident photon energy (hυ) is given by Tauc's relation:

$$(\alpha h\nu) = A(h\nu - E_g)^n \qquad (1)$$

where *hv* is photon energy, *A* is constant, α is absorption coefficient while n depends on the nature of the transition. For direct transitions n = ½ or ⅔, while for indirect ones n = 2 or 3, depending on whether they are allowed or forbidden, respectively. The best fit of the experimental curve to a band gap semiconductor absorption function was obtained for n = ½. These graphs extrapolated to *hv* axis give the values of E_g as 2.7 eV for the as-grown film and 2.6 eV for the annealed film, as we observe them in Figure 6b. The band gap shift of CdS after heat treatment could be explained in terms of nanosized effect of the as-deposited film [35]. The estimated direct optical band gap (annealed and unannealed) did not agree with the 2.4eV reported in the literature [23,33,34]. This variation may be due to post-isothermal conditions of CdS buffer layer.

3.4 Solar cell properties

Solar cells with a device structure of ITO/i-ZnO/CdS/$CuInS_2$/Mo/SLG were prepared by depositing CdS and ZnO/ITO layers on $CuInS_2$. Table 1 and 2 reveal the annealing effect and annealing-time dependence of solar cell performance of the device. From Table 1, sample #1 with CdS layer annealed in air at 200^{o}C for 30min and unannealed ZnO layer reveals a better power-conversion efficiency (0.092%) with the following characteristics (open circuit voltage, V_{oc} = 28mV , short-circuit current density, J_{sc} = 14.25mA/cm^2 and fill factor, *FF* = 0.23). When both layers (i.e CdS and ZnO/ITO) were annealed (200^{o}C, 30min and 150^{o}C respectively), no efficiency was deduced from sample #2. Sample #4 had both layers unannealed with efficiency ≈ 0.052%, open circuit voltage, V_{oc} = 32mV, short-circuit current density, J_{sc} = 6.41mA/cm^2 and fill factor, *FF* = 0.26.

Table 1: Solar cell performances with different annealing conditions on bi-layer structures of CdS and ZnO

Sample	CdS	ZnO	η[%]	Voc[mV]	Jsc[mA/cm2]	FF
①	annealed in air 200°C, 30min	w/o annealing	0.092	28	14.25	0.23
②		150°C	not having conversion efficiency			
③	w/o annealing		0.031	14	9.58	0.23
④		w/o annealing	0.052	32	6.41	0.26

Table 2: Solar cell performances showing annealing-time dependence of CdS buffer layer

Sample	CdS	η[%]	Voc[mV]	Jsc[mA/cm2]	FF
①	without annealing	0.023	13.7	7.47	0.23
②	annealed in air 200° C, 10min	0.32	134	8.24	0.29
③	annealed in air 200° C, 20min	0.011	8.4	5.32	0.24
④	annealed in air 200° C, 30min	0.092	28	14.25	0.23

Generally, comparing sample #1 with sample #4, it could be seen that annealing the CdS improved the cell performance. The improvement is seen in the current density J_{sc} which is as a result of improved crystal quality of CdS. However the open circuit voltage V_{oc} and the fill factor *FF* was reduced as a result of too much Cd ion diffusing into the CIS. Hence there is need to balance the Cd ion diffusion and improvement of CdS quality. In addition, comparing sample #3 with sample #4 and sample #1 with sample #2 respectively, we deduced that ZnO should be deposited without heat treatment and that too much annealing of CdS is not good for the cell performance to avoid too much Cd ion diffusion into the CIS. There is need for optimization to

obtain a balance between the crystal quality and Cd ion diffusion in order to get the best cell performance. The performance of the cells is illustrated in figure 7 based on the crystal quality and the Cd ion diffusion.

We annealed some samples in air at 200^{o}C after the deposition of CdS and varied the annealing time from 10-30min. The cell structure has ZnO layer unannealed throughout the investigation and the result is shown in table 2. Sample #1 with bi-layer of unannealed CdS and ZnO has a power-conversion efficiency of 0.023%, V_{oc} = 13.7mV, J_{sc} = 7.47mA/cm^2 and *FF* = 0.23. The maximum cell performance was obtained for sample #2. There was a remarkable improvement in open-circuit voltage, V_{oc} and short circuit current density, J_{sc} except for sample #3 where 8.4mV and 5.32mA/cm^2 was recorded respectively for V_{oc} and J_{sc}. The rough surface morphology of the CIS film results in enlargement of interface areas between the CdS buffer and CIS absorber, thus limiting V_{oc} and *FF* of the cell [36]. Generally, there was moderate diffusion of Cd ions into CIS.

4. Conclusion

CdS/$CuInS_2$ thin film solar cells have been fabricated and annealing time effect on the solar performance studied. XRD showed a hexagonal structure for the n-type CdS buffer layer. The thermal treatment reduced the roughness from 28.8 to 16.4nm while optical absorption reveals a high transmittance ≥ 80%. CIS solar cell with a CdS buffer layer annealed at 200^{o}C for 10min showed an efficiency of 0.32% (V_{oc} = 134mV, J_{sc} = 8.24mA/cm^2 and *FF* = 0.29). The efficiency of annealed sample is about 0.297% larger than that of unannealed sample. For a bi-layer of CdS and ZnO, it was observed that the bi-layer shows a better performance (η = 0.092%, V_{oc} = 28mV, J_{sc} = 14.25mA/cm^2 and *FF* = 0.23) when compared with unannealed ZnO layer. Hence, diffusion of Cd ions into CIS is as a result of too much annealing. We can establish that for good cell performance, the CdS be annealed such that the effect of improvement in crystal quality be greater than the effect of Cd diffusion.

Acknowledgement

The authors thank S. Yamaguchi, Y. Yamaguchi, and S-W Chang for their assistance in conducting the experiments. This work was supported in part by the Research Center for Green and Safety Sciences, and the Photovoltaic Science and Technology Research Division, under the Research Institute for Science and Technology, Tokyo University of Science. Fabian I. Ezema thanks immensely Prof. Kohei Soga for inviting him to use his laboratory as Matsumae International Foundation (MIF) research fellow and for giving him unhindered visit to Sugiyama Lab. Fabian I. Ezema is grateful to Matsumae International Foundation (MIF) for fellowship award at Tokyo University of Science, Japan.

References

[1] J. Britt, C. Ferekides, Appl. Phys. Lett. **62**, 2851 (1993).
[2] S. Wagner, J. L.Shay, P. Migliorato, H. M. Kasper, Appl. Phys. Lett. **25**, 434 (1974).
[3] W.N. Shafarman, L. Stolt, Cu(InGa)Se2 Solar Cells. in: Luque A, Hegedus S (Eds.). Handbook of Photovoltaic Science and Engineering. John Wiley & Sons Ltd, Hoboken, (2003).
[4] M. Powalla, P. Jackson, W. Witte, D. Hariskos, S. Paetel, C. Tschamber, W. Wischmann Sol Energy Mater & Sol Cells **119**, 51 (2013).
[5] S. Bandyopadhyaya, S. Chaudhuri, A.K. Pal, Solar Energy Materials and Solar Cells **60**, 323 (2000).
[6] C.V. Klopmann, J. Djordjevic, E. Rudigier, R. Scheer, J Crystal Growth **289**, 121 (2006).
[7] J. Klaer, R. Klenk, H-W. Schock, Thin Solid Films **515**, 5929 (2007).

[8] J. Klaer, J. Bruns, R. Henninger, K. Siemer, R. Klenk, K. Ellmer, D. Bräunig, Semiconductor Sci and Tech **13**, 1456 (1998).
[9] K. Siemer, J. Klaer, I. Luck, J. Bruns, R. Klenk, D. Bräunig, Sol Energy Materials and Solar Cells **67**, 159 (2001).
[10] M. Krunks, O. Bijakina, T. Varema, V. Mikli, E. Mellikov, Thin Solid Films **338**, 125 (1999).
[11] R. Klenk, J. Klaer, R. Scheer, M.C. Lux-Steiner, I. Luck, N. Meyer, U. Rühle, Thin Solid Films **480–481**, 509 (2005).
[12] C.J. Hibberd, E. Chassaing, W. Liu, D.B. Mitzi, D. Lincot, A.N.Tiwari, Progress in Photovoltaics: Research and Applications **18**, 432 (2010).
[13] I. Oja, M. Nanu, A. Katerski, M. Krunks, A. Mere, J. Raudoja, A. Goossens, Thin Solid Films **480–481**, 82 (2005).
[14] M. Krunks, O. Kijatkina, A. Mere, T. Varema, I. Oja, V. Mikli, Solar Energy Materials and Solar Cells **87**, 207 (2005).
[15] A. Katerski, A. Mere, V. Kazlauskiene, J. Miskinis, A. Saar, L. Matisen, A. Kikas, M. Krunks, Thin Solid Films **516**, 7110 (2008).
[16] C. Camus, N.A. Allsop, S.E. Gledhill, W. Bohne, J. Röhrich, I. Lauermann, M.C. Lux-Steiner, C.H. Fischer, Thin Solid Films **516**, 7026 (2008).
[17] S. Nakamura and A. Yamamoto, Solar Energy Materials and Solar Cells **49**, 415 (1997).
[18] B. Asenjo, A.M. Chaparro, M.T. Gutiérrez, J. Herrero, Thin Solid Films **511–512**, 117 (2006).
[19] S. Nakamura and A. Yamamoto, Solar Energy Materials and Solar Cells **75**, 81 (2003).
[20] R.C. Valderrama, M. Miranda-Hernández, P.J. Sebastian, A.L. Ocampo, Electrochimica Acta **53**, 3714 (2008).
[21] Q. Huang, K. Reuter, S. Amhed, L. Deligianni, L.T. Romankiw, S. Jaime, P-P. Grand, V. Charrier, J. Electrochem Soc. **158**, D57 (2011).
[22] M. Sugiyama, C. Fujiwara, R. Shoji, S.F. Chichibu, J. of App Physics **50**, 065503 (2011).
[23] Y. Chung, D. Cho, N. Park, K. Lee, J. Kim, Current Applied Physics **11**, S65 (2011).
[24] R. Ortega-Borges and D.Lincot, J Electrochem Soc. **140**, 3464 (1993).
[25] K.C. Wilson, E. ManiKandan, M.B. Ahamed, B.W.Mwakikunga, J Alloys & Compounds **585**, 555 (2014).
[26] K.B. Jinesh, K.C. Wilson, S.V. Thampi, C.S. Kartha, K.P. Vijayakumar, T. Abe, Y. Kashiwaba, Physica E **19**, 303 (2003).
[27] P. Zhao and K. Hung, Cryst Growth Design **8**, 717 (2008).
[28] T. Zhai, X. Fang, L. Li, Y. Bando, D. Golberg, Nanoscale **2,** 168–87 (2010).
[29] E. Moons, D. Gal, J. Beier, G. Hodes, D. Cahen, L. Kronik, L. Burstein, B. Mishori, Y. Shapira, D. Hariskos, H.W. Schock, Sol Energ Mater & Sol Cells **43**, 73 (1996).
[30] T. Sakurai, N. Ishida, S. Ishizuka, M.M. Islam, A. Kasai, K. Matsubara, K. Sakurai, A. Yamada, K. Akimoto, S. Niki, Thin Solid Films **516**, 7036 (2008).
[31] W. Bohua, Z. Shichao, F. Hua, L. Wenbo and. D. Zhijia, Materials Chemistry and Physics, DOI:10.1016/j.matchemphys.2011.09.051, (2011).
[32] F. I. Ezema, D. D. Hile, S. C. Ezugwu, R. U. Osuji, P. U. Asogwa, Journal of Ovonic Research **6**, 99 (2010).
[33] J. Han, C. Spanheimer, G. Haindl, G. Fu, V. Krishnakumar, J. Schaffner, C. Fan, K. Zhao, A. Klein, W. Jaegermann, Sol Energy Mater & Sol Cells **95**, 816 (2011).
[34] M. Rusu, A. Rumberg, S. Schuler, S. Nishiwaki, R. Wu¨rz, S.M. Babu, M. Dziedzina, C. Kelch, S. Siebentritt, R. Klenk, T. Schedel-Niedrig, M.C. Lux-Steiner, J. Phys. Chem. Solids **64**, 1849 (2003).
[35] J. Hiie, T. Dedova, V. Valdna, K. Muska, Thin Solid Films **511-512**, 443 (2006).
[36] S.M. Lee, S. Ikeda, Y. Otsuka, W. Septina, T. Harada, M. Matsumura, Electrochimica Acta **79**, 189 (2012).